The structure of 4-methylphenol and its water cluster revealed by rotationally resolved UV spectroscopy using a genetic algorithm approach

Grzegorz Myszkiewicz and W. Leo Meerts[a]
*Molecular and Biophysics Group, Institute for Molecules and Materials, Radbound University Nijmegen,
P.O. Box 9010, NL-6500 GL Nijmegen, The Netherlands*

Christian Ratzer and Michael Schmitt[b]
Institut für Physikalische Chemie, Heinrich-Heine-Universität 40225 Düsseldorf, Germany

The structure of 4-methylphenol (*p*-cresol) and its binary water cluster have been elucidated by rotationally resolved laser-induced fluorescence spectroscopy. The electronic origins of the monomer and the cluster are split into four sub-bands by the internal rotation of the methyl group and of the hydroxy group in case of the monomer, and the water moiety in case of the cluster. From the rotational constants of the monomer the structure in the S_1 state could be determined to be distorted quinoidally. The structure of the *p*-cresol-water cluster is determined to be *trans* linear, with a O–O hydrogen bond length of 290 pm in the electronic ground state and of 285 pm in the electronically excited state. The S_1-state lifetime of *p*-cresol, *p*-cresol-d_1, and the binary water cluster have been determined to be 1.6, 9.7, and 3.8 ns, respectively. © *2005 American Institute of Physics*. [DOI: 10.1063/1.1961615]

I. INTRODUCTION

In the present study we present the determination of the geometry of *p*-cresol and its binary water cluster in the ground state and the electronically excited S_1 state by means of rotationally resolved electronic spectroscopy. The determination of excited state structures of aromatic molecules gives insight into the changes of the electronic properties of the chromophore. In a series of investigations, we determined the structural changes of some *para*-disubstituted aromatic molecules such as *p*-fluorophenol,[1] *p*-cyanophenol,[2] and *p*-methylstyrene.[3] In all these cases a quinoidal distortion along the *a* axis of the molecule is found, whereas for singly substituted benzenes a symmetric distortion (benzenoid) of the aromatic ring is found.[4] Changes of the electronic properties are also reflected in the change of the torsional barriers of symmetric (e.g., CH_3) or asymmetric tops (e.g., OH), which are directly attached to the benzene ring. In recent publications it was shown how the different electronic properties of the fluorine and the cyanogroup influence the barrier to hydroxy torsion in both electronic states of *p*-fluorophenol and *p*-cyanophenol.[1,2]

4-methylphenol possesses two feasible large amplitude motions: the methyl rotation with a mixed V_3/V_6 potential and the twofold hydroxy rotation. The molecular symmetry group that describes both motions is G_{12}. In the *p*-cresol-water cluster, the OH torsion is quenched; instead an additional splitting due to the torsional motion of the water moiety with respect to the water symmetry axis is observed. This barrier is expected from the similar phenol-

water system to be quite low. Thus, we have the case of twolow barrier torsional motions, which will split the origin into four sub-bands, an $A^{(3)}$-E pair due to the threefold motion and an $A^{(2)}$-B pair due to the twofold rotation. We use the superscripts (2) and (3) to distinguish the different A sublevels from the two- and threefold internal rotation from the A rotational constant. Since the rotational constants of this cluster are quite small, the overlapping of four subspectra leads to a very-congested overall spectrum in which it is difficult, if not impossible, to identify single rovibronic lines. However, the assignment of well-resolved lines to specific quantum numbers of the transitions is an indispensable prerequisite for an assigned fit of the molecular parameters. We have shown recently that in these cases of many overlapping lines, the use of a genetic algorithm approach for automated assignment of the spectra simplifies the interpretation and in many cases only makes it possible.[5]

4-methylphenol has found considerable interest as a chromophore and simple molecular model of the aromatic amino acid tyrosine.[6] Proton transfer, electron transfer, and hydrogen transfer are important processes in clusters of tyrosine. E.g., in the water oxidizing complex of photosystem II, tyrosine is oxidized and reduced by hydrogen atom transfer involving tyrosine, water, and histidine in the active center.[7]

The electronic ground state of *p*-cresol has been investigated by infrared[8,9] and Raman spectroscopy,[6,10] by stimulated emission dip spectroscopy,[11] and by dispersed fluorescence spectroscopy.[12] Recently Lin *et al.* presented a mass-analyzed threshold ionization spectrum of the *p*-cresol cation.[13] The nature of conformational preferences in *p*-cresol has been studied theoretically by Richardson *et al.*[14] They determined the most stable conformation of *p*-cresol on

---

[a]FAX: +33 24 356 3311; electronic mail: leo.meerts@science.ru.nl
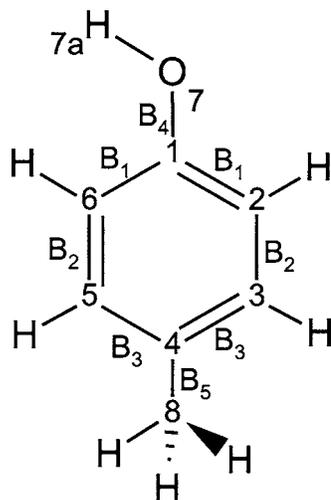[b]FAX: +49 211 81 15195; electronic mail: mschmitt@uni-duesseldorf.de

FIG. 1. The most stable conformation and atomic numbering of *p*-cresol.

MP2 level of theory to be eclipsed with respect to the methyl-group orientation, and the OH group on the same side of the aromatic ring as the eclipsed methyl hydrogen (*syn*), c.f. Fig. 1.

Several *p*-cresol-water clusters with up to four water molecules have been studied using dispersed fluorescence and- resonant two-photon ionization (R2PI) spectroscopy in the region of the intermolecular vibrations.[15,16] From the vibrational analysis it is deduced that the binary cluster is hydrogen bound via a *trans*-linear H bond as in the similar phenol-water system.[17]

II. EXPERIMENTAL SETUP

The experimental setup for high-resolution laser-induced fluorescence (LIF) is described in detail elsewhere.[18] Briefly, the molecular-beam machine consists of three differentially pumped vacuum chambers that are linearly connected by two skimmers with orifice diameters of 1 mm (first chamber) and 2 mm (second chamber) for the reduction of the Doppler width to 25 MHz. The expansion chamber is evacuated by a 8000-l/s oil diffusion pump (Leybold DI 8000), which is backed by a 250-m^3/h roots blower pump (Saskia RPS 250) and a 65-m^3/h rotary pump (Leybold D65B). The second chamber serves as a buffer chamber and is pumped by a 400-l/s turbo-molecular pump (Leybold Turbovac 361), backed by a 40-m^3/h rotary pump (Leybold D40B), maintaining a chamber pressure below 1×10^{-5} mbar. The third chamber is pumped by a 145-l/s turbo-molecular pump (Leybold Turbovac 151) through a liquid-nitrogen trap and backed by a 16-m^3/h rotary pump (Leybold D16B) resulting in a vacuum better than 1×10^{-6} mbar. The molecular beam is crossed at right angles with the laser beam 360 mm downstream from the nozzle.

The laser system consists of a ring dye laser (Coherent 899-21), which is pumped with 6 W of the 514-nm line of an Ar$^+$-ion laser (Coherent Innova 100). This light is coupled into an external-folded ring cavity (Spectra Physics) for second-harmonic generation (SHG). Typical UV powers are 10–40 mW. The laser-induced fluorescence is collected perpendicular to the plane defined by the laser and molecular

beam by an imaging optics setup consisting of a concave mirror and two plano-convex lenses. Data acquisition is performed and synchronized by means of a home-built real time LINUX program.[19]

III. THEORY OF THE INTERNAL ROTATION

The coupling between the internal rotation of the methyl group and the overall rotation of the molecule and the coupling of the OH and the water torsion with the overall rotation are treated in the formalism of the principal axis method (PAM).[20,21] This is exact in the first (symmetric-top) case, but only an approximation for the twofold (asymmetric) top. Nevertheless as the hydrogen atom of the OH group and in the water moiety is light, and the inertial axes remain virtually unchanged during rotation of the top, the application of the PAM leads to reliable results. The Hamiltonian for the rotation-torsion interaction can be written as

$$\hat{H} = \hat{H}_R + \hat{H}_T + \hat{H}_{\text{RT}} \tag{1}$$

with the rigid rotational Hamiltonian given by

$$\hat{H}_R = AJ_a^2 + BJ_a^2 + CJ_c^2. \tag{2}$$

The torsional Hamiltonian for the mixed V_3/V_6 potential (methyl torsion) is given by

$$\hat{H}_T = Fp^2 + \frac{1}{2}\sum_{n=1}^{2} V_{3n}(1 - \cos 3n\alpha), \tag{3}$$

and for a twofold V_2 potential (OH and water torsion) by

$$\hat{H}_T = F\rho^2 + \frac{1}{2}\sum_{n=1}^{2} V_{2n}(1 - \cos 2n\alpha). \tag{4}$$

F is the torsional constant and defined by

$$F = \frac{h}{8\pi^2 r I_\alpha} \tag{5}$$

with

$$r = 1 - \sum_{g=a,b,c} \frac{\lambda_g^2 I_\alpha}{I_g}. \tag{6}$$

Here the λ_g ($g=a,b,c$) are the direction cosines between the inertial axes and the axis of internal rotation. I_α is the moment of inertia of the internal rotor with respect to its symmetry axis and I_g are the principal moments of inertia of the entire molecule. In what follows, the treatment for the $n=2$ and $n=3$ potentials is identical.

The coupling of internal and overall rotation is described by $\hat{H}_{\text{RT}}$:[20,22]

$$\hat{H}_{\text{RT}} = FW_{v\sigma}^{(1)}(\rho_a J_a + \rho_b J_b + \rho_c J_c) + FW_{v\sigma}^{(2)}(\rho_a J_a + \rho_b J_b + \rho_c J_c)^2, \tag{7}$$

where the first-order perturbation coefficients $W_{v\sigma}^{(1)}$ are zero for the nondegenerate $A^{(2)}$, $A^{(3)}$, and B levels. $W_{v\sigma}^{(2)}$ is nonzero for all levels.

The coefficients ρ_g with $g = a, b, c$ are defined as

$$\rho_a = I_\alpha / I_a \cos \eta,$$

$$\rho_b = I_\alpha / I_b \sin \eta, \tag{8}$$

with η as the angle between the projection vector of the n-fold rotor axis on the ab plane and the a axis.

The nth-order perturbation coefficients $W_{v\sigma}^{(n)}$ in Eq. (7) are defined by[20]

$$W_{v\sigma}^{(0)} = \frac{E_{v\sigma}}{F}, \tag{9}$$

$$W_{v\sigma}^{(1)} = -2\langle v, \sigma | p | v, \sigma \rangle, \tag{10}$$

$$W_{v\sigma}^{(2)} = 1 + 4F \sum_{v'} \frac{|\langle v, \sigma | p | v', \sigma \rangle|^2}{E_{v\sigma} - E_{v'\sigma}}, \tag{11}$$

where $|v, \sigma\rangle$ are eigenfunctions of Eqs. (3) and (4), and $E_{v\sigma}$ are the respective eigenvalues with v as the torsional state index.

IV. THE GENETIC ALGORITHMS

The experimental spectra were assigned automatically using a genetic algorithm-based fit described in detail in Refs. 5 and 23. We used the genetic algorithm (GA) library PGAPACK version 1.0, which can run on parallel processors.[24] The calculations were performed on eight processors of a SUN UltraSPARC 333 MHz and on a 2.6-GHz personal computer (PC) with two processors under LINUX. The genetic algorithm uses concepts copied from natural reproduction and selection processes. For a detailed description of the GA the reader is referred to the original literature on evolutionary or genetic algorithms.[25–27] In the present work a population of 300 was used and the calculation was completely converged after 500 generations. The other parameters which control the genetic algorithm convergency are similar as in Ref. 5.

The cost function used to describe the quality of the fit was defined as $C_{fg} = 100(1 - F_{fg})$ with the fitness function F_{fg}:

$$F_{fg} = \frac{(\mathbf{f}, \mathbf{g})}{\|\mathbf{f}\| \|\mathbf{g}\|}. \tag{12}$$

$\mathbf{f}$ and $\mathbf{g}$ represent the experimental and calculated spectra, respectively, and the inner product $(\mathbf{f}, \mathbf{g})$ is defined with the metric $\mathbf{W}$, which has the matrix elements $W_{ij} = w(|j - i|) = w(r)$ as

$$(\mathbf{f}, \mathbf{g}) = \mathbf{f}^T \mathbf{W} \mathbf{g}, \tag{13}$$

and the norm of $\mathbf{f}$ as $\|\mathbf{f}\| = \sqrt{(\mathbf{f}, \mathbf{f})}$ and similar for $\mathbf{g}$. For $w(r)$ we used a triangle function[23] with a width of the base of Δw:

$$w(r) = \begin{cases} 1 - |r| \left(\frac{1}{2} \Delta w \right) & \text{for } |r| \leq \frac{1}{2} \Delta w \\ 0 & \text{otherwise}. \end{cases} \tag{14}$$

Since the GA performs an intensity fit of the complete spectrum, much better information on the transition dipole moment (TDM) orientation and linewidth parameters are
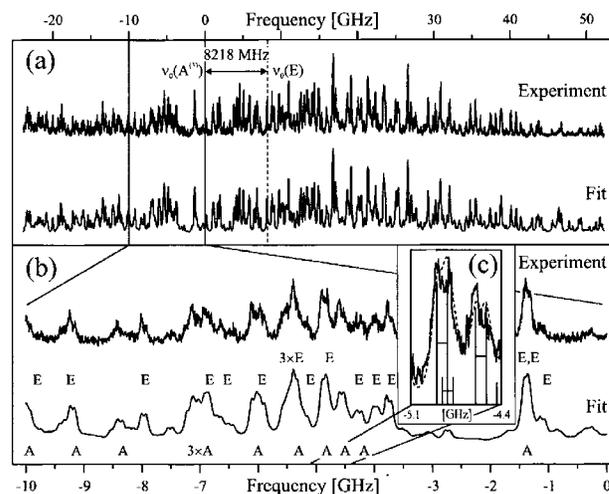

FIG. 2. (a) Experimental and fitted rovibronic spectrum of the electronic origin of 4-methylphenol. (b) 10-GHz zoom of the (a) spectrum. (c) Inset showing three pairs of rovibronic transitions split by the twofold hydroxy group rotation in cresol. For the sake of clarity only the strongest transitions are shown and the splitting is marked with the horizontal lines. The solid line represents the experiment and the dashed line, the fit. All frequencies are given relative to the electronic origin at 35 331.257(10) cm^{-1}.

gathered than from an intensity fit to a few individual lines. Thus, the GA results in improved values for the in plane angle θ of the TDM and also of the Lorentzian width of the individual rovibronic lines. Therefore, excited state lifetimes can be determined with a much higher accuracy than in line-shape fits of individual rovibronic lines.

V. RESULTS AND DISCUSSION

A. 4-methylphenol

Figure 2 shows the rotationally resolved LIF spectrum of the electronic origin of p-cresol. The spectrum is a pure b-type spectrum. It is split into two components, $A^{(3)}$ and E by the internal rotation of the methyl group $(E_{v,0} - E_{v,\pm 1})$. Their respective origins, which are 8218 MHz apart, are marked arrows.

In two recent publications[3,28] we showed how a combined fit to high-resolution rovibronic data and low-resolution torsional transitions can be used to improve the determination of the barriers and torsional constants in both electronic states. A, B, C, V_3, V_6, F, and η were fitted for each electronic state to the rotationally resolved origin and to the torsional transitions from Ref. 29. These torsional transitions are obtained from the zero-order perturbation coefficient, c.f. Eq. (9). The rovibronic spectrum was fitted using the genetic algorithm (GA) approach, described in Ref. 5. The parameters that determine the intensity and line form are the rotational temperatures, the Lorentzian and Gaussian linewidths, and the projections of the transition dipole moment on the inertial axes. They can be fitted most favorably using the GA algorithm. The Lorentzian contribution to the linewidth of the Voigt profile with a fixed Doppler width of 25 MHz is determined to be 100 ± 10 MHz, equivalent to a S_1-state lifetime of 1.6 ± 0.2 ns. The results of the fits are compiled in Tables I and II.

TABLE I. Molecular parameters of 4-methylphenol and 4-methyl[7D]phenol from the GA fit. The ground-state rotational constants of 4-methylphenol have been kept fixed at the microwave values from Ref. 30.

4-methylphenol		S_0	S_1
A	(MHz)	5494.570	5154.6(12)
B	(MHz)	1456.963	1470.51(67)
C	(MHz)	1160.200	1153.62(41)
V_3	(MHz)	18.00(25)	7.99(34)
V_6	(MHz)	−13.8(45)	−24.7(43)
F	(cm⁻¹)	5.224(98)	5.108(98)
ν_0	(cm⁻¹)	35 331.257(10)	
$\nu_0(E) - \nu_0(A^{(3)})$	(MHz)	8218(16)	
$\nu_0(A^{(2)}) - \nu_0(B)$	(MHz)	90(13)	
4-methyl[7D]phenol			
A	(MHz)	5442.16(94)	5110.04(94)
B	(MHz)	1417.59(37)	1431.03(37)
C	(MHz)	1133.45(27)	1127.46(27)
V_3	(MHz)	18.00(25)	7.99(34)
V_6	(MHz)	−13.8(45)	−24.7(43)
F	(cm⁻¹)	5.170(7)	5.066(7)
ν_0	(cm⁻¹)	35 326.729(10)	
$\nu_0(E) - \nu_0(A^{(3)})$	(MHz)	8656.2(50)	

Closer inspection of the spectrum shows that each of the rovibronic transitions is further split into two close lying sub-bands [c.f. Fig. 2(c)] due to the hindered –OH torsion. As a twofold torsion leads only to nondegenerate $A^{(2)}$ ($\sigma=0$) and B ($\sigma=1$) levels, the first-order perturbation coefficients from Eq. (10) are zero. The second-order perturbation coefficients which are nonzero [Eq. (11)] are quadratic in the angular momentum and can therefore be incorporated in the rotational constants. Since the OH-torsional barrier is very high, the perturbations are small and both sub-bands can be fitted with the same set of effective rotational constants and an origin shift between the $A^{(2)}$ and B bands of 90 MHz.

Determination of barriers and torsional constants in both electronic states demands more information from other spectroscopic techniques. In the microwave spectrum a splitting of the b-type transitions of 175 MHz has been observed.[30] The selection rule for b-type transitions is $\Delta\sigma=\pm1$, so that the splitting between the subtorsional levels amounts to 87.5 MHz. The frequency of the pure torsional transition has

TABLE II. Torsional transitions of 4-methylphenol. The electronic transitions are labeled by the m quantum number and the symmetry of the subtorsional level σ: $m\sigma(S_1) \leftarrow m\sigma(S_0)$ for absorption bands and $m\sigma(S_1) \rightarrow m\sigma(S_0)$ for emission bands.

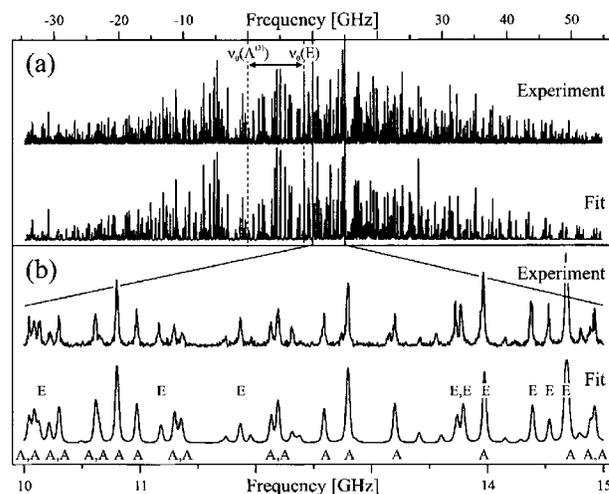| p-cresol	Exp.[29]	Fit.	Diff.	
$1e \leftarrow 1e$	8218(16)	8214	−4	MHz
$2e \leftarrow 1e$	15.1(5)	15.4	+0.3	cm⁻¹
$3a_1 \leftarrow 0a_1$	51.7(5)	52.7	+1.0	cm⁻¹
$4e \leftarrow 1e$	77(2)	77.9	+0.9	cm⁻¹
$5e \leftarrow 1e$	125(2)	123.6	−1.4	cm⁻¹
$1e \rightarrow 2e$	18.5(10)	17.7	−0.8	cm⁻¹
$0a_1 \rightarrow 3a_1$	52.5(10)	51.9	−0.6	cm⁻¹
$1e \rightarrow 4e$	80.0(20)	80.1	+0.1	cm⁻¹

FIG. 3. Rovibronic spectrum of the electronic origin of 4-methyl[7D]phenol. Frequencies are given relative to the electronic origin at 35 326.729(10) cm⁻¹.

been determined by IR spectroscopy to be 294 cm⁻¹.[9] The first overtone of the torsional vibration in the electronically excited state is determined to be 1199 cm⁻¹. Using these transitions and fixing the torsional constant F at 690 GHz (the value in phenol), we are able to fit the ground-state torsional V_2 barrier to 1130 cm⁻¹ and the excited state barrier to 4395 cm⁻¹. Both values are slightly lower than the corresponding values in phenol (1215 and 4710 cm⁻¹, respectively).[17]

B. 4-methyl[7-*D*]phenol

Figure 3 shows the rotationally resolved LIF spectrum of the electronic origin of 4-methyl[7-*D*]phenol. The spectrum is a pure b-type spectrum. Due to the heavier OD group, the twofold torsion is quenched in this system and the molecular symmetry group for the description of the molecule is G_6. Consequently, the origin band consists only of a split pair of $A^{(3)}$ and E bands with a frequency spacing of 8656 MHz.

Table I gives the molecular parameters that have been determined using the GA program. The lifetime for 4-methyl[7-*D*]phenol is determined to be 9.7±0.6 ns from a Lorentzian contribution to the total linewidth of 16.4±1 MHz. The $A^{(3)}E$ subtorsional splitting is very similar to the splitting in 4-methylphenol, also indicating similar potential barriers. As no torsional bands of 4-methyl[7-*D*]phenol have been measured not enough data are available to fit the barriers to methyl rotation in this molecule. Nevertheless, since the effect of hydroxy deuteration on the methyl barrier is supposed to be small, we set barriers and torsional constants equal to those of 4-methylphenol.

C. 4-methylphenol (H₂O)₁

Figure 4 presents the rotationally resolved electronic spectrum of the origin of the p-cresol-water cluster at 34 972.873 cm⁻¹. The origin is split into an $A^{(3)}$ and an E sub-band due to the methyl torsion with a subtorsional splitting of 5459 MHz and into an $A^{(2)}$ and B sub-band due to the water torsion with a subtorsional splitting of 29 428 MHz.
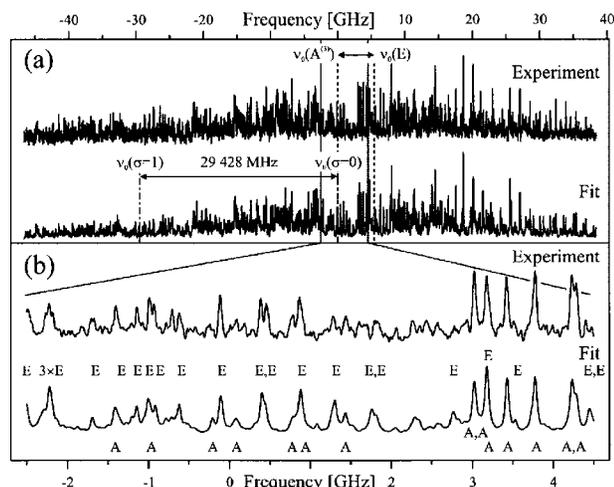
FIG. 4. Rovibronic spectrum of the electronic origin of 4-methylphenol water. Frequencies are given relative to the electronic origin at 34 972.873(10) cm^{-1}.

The angle of the transition dipole moment with the a axis is determined from the relative intensities of a and b bands to be 76.70°. The rotation of 13.3° with respect to the monomer is in good agreement with a value of 20°, that is predicted by rotation of the inertial axis upon cluster formation on the basis of the *ab initio* structure.

As in the case of phenol, the subtorsional structure due to the twofold water torsion can be fit using a rigid-rotor model with different rotational constants for both components. Similar to the phenol-water case, the B and C rotational constants of the ($\sigma=0$) and ($\sigma=1$) components are equal within their uncertainties. The A constants of the subtorsional components differ by about 11 MHz, indicating that the torsional axis of the water torsion is more or less parallel to the main inertial a axis of the cluster. This structure can be described as a *trans*-linear hydrogen bond configuration, with the water moiety acting as proton acceptor, like in phenol water. A spin statistics of 1:3 for the ratio of ($\sigma=0$) to ($\sigma=1$) further supports a structure with the water moiety symmetric with respect to the aromatic plane.

This analysis clearly shows the convenience of the GA analysis of such a complex spectrum. Although by eye no periodicity can be observed at first glance, the GA is capable of easily finding the two splittings from the methyl torsion

(5459 MHz) and the water torsion (29 428 MHz). Of course, the application of the GA-based-automated technique still requires the choice of the "correct" Hamiltonian for the problem under consideration. An easy way of finding spectral splittings (and thus obtaining information about the required Hamiltonian) is to perform an autocorrelation of the spectrum. This method has been shown by Helm *et al.* to be helpful in the analysis of the phenol-water cluster spectrum[31] and later by Remmers *et al.* in the analysis of the tunneling spectrum of the benzoic acid dimer.[32] Nevertheless, if one component of the complete spectrum amounts to more than 50% of the total intensity, the GA is capable of fitting this part of the spectrum, although it might be concealed in the dense spectrum of other component(s) and would therefore be inaccessible to a classical analysis using line-position-assigned fits. From the difference of the partly fitted spectrum to the experimental one, the missing components can easily be recognized and subsequently fitted.

In order to compute the geometrical rotational constants from the torsionally perturbed constants of Table III, we have to estimate the V_2 potential energy barrier and the torsional constant F for the water torsion in both electronic states. However, only three pieces of information are available for the determination of these four parameters: the ($\sigma=0$)/($\sigma=1$) subtorsional splitting of 29 428 MHz, and the difference of the A rotational constants for ($\sigma=0$) and ($\sigma=1$) in the electronic ground state and in the electronically excited state. Fixing F'' of the ground state to the value determined for phenol water[28] (14.813 cm^{-1}) (the ground-state acidities of phenol and cresol are similar, therefore one would expect similar torsional constants for the water moiety), a ground-state barrier V_2'' of 182.6 cm^{-1}, an excited state barrier V_2' of 125.3 cm^{-1}, and a torsional constant F' in the excited state of 14.9 cm^{-1} are calculated. These values are very close to the torsional barriers of phenol water.

D. Determination of the structures

The program *pKrFit* (Ref. 4) was used to determine the structure of 4-methylphenol in the S_0 and S_1 states from the rotational constants of the two isotopomers described above. Due to the limited number of isotopomers in this study, we performed a fit to the r_0 structure, which completely neglects the vibrational contributions from the different isotopomers.

TABLE III. Molecular parameters of 4-methylphenol water.

		S_0		S_1	
		$\sigma=0$	$\sigma=1$	$\sigma=0$	$\sigma=1$
A	(MHz)	3663.48(244)	3652.19(53)	3590.87(244)	3576.37(53)
B	(MHz)	765.60(59)	765.98(31)	774.78(59)	774.35(31)
C	(MHz)	637.00(48)	637.71(31)	640.76(48)	641.61(31)
V_3	(MHz)	18.00(25)		7.99(34)	
V_6	(MHz)	−13.8(45)		−24.7(43)	
F	(cm^{-1})	5.41(7)		5.21(7)	
η	(°)	19.1(10)		19.1(10)	
ν_0	(cm^{-1})			34 971.891(10)	34 972.873(10)
$\nu_0(A^{(2)})-\nu_0(B)$	(MHz)		29 428(7)		
$\nu_0(A^{(3)})-\nu_0(E)$	(MHz)		5459(6)		

TABLE IV. Structural r_0 parameters of *p*-cresol. For atomic numbering see Fig. 1. All values are in pm.

	$B_1(C_1C_2)$	139.9(1)
	$B_2(C_2C_3)$	140.5(3)
S_0	$B_3(C_3C_4)$	138.9(1)
	$B_4(CO)$	138.3(6)
	$B_5(CC_{methyl})$	151.3(6)
	$B_1(C_1C_2)$	142.2(10)
	$B_2(C_2C_3)$	138.1(10)
S_1	$B_3(C_3C_4)$	144.3(4)
	$B_4(CO)$	134.5(11)
	$B_5(CC_{methyl})$	150.3(2)

A simple model for the geometry has been adopted, that is given in Fig. 1. All aromatic CH bonds are set to the same value (107.7 pm for the ground state and 107.4 pm for the excited state), the CH bonds of the methyl group are fixed at 109.0 pm. The OH bond lengths from the structural fits of phenol have been taken as constants (96 pm in the S_0 and 99 pm in the S_1 states). Opposing CC bonds are set equal.

Table IV gives the results for the fits of the S_0 and the S_1 structure. The aromatic ring expands upon electronic excitation quinoidally, as has been found for other *para*-disubstituted aromatic compounds. The CO and the CC_{methyl} bond lengths decrease, which are in agreement with a quinoidal distortion of the ring system. The relative shortening of these bands cannot be determined accurately, as both bonds nearly coincide with the main inertial *a* axis. Because the deuteration is at a position close to this axis, both bond lengths are strongly correlated. The results present therefore only one possible combination of the bond length decreases.

From the above determined S_0 and S_1 structures of the cresol moiety, we fitted the structure of the *p*-cresol water to the geometric rotational constants. All geometry parameters in *p*-cresol have been kept fixed at the monomer values, the geometry of the water moiety has also been kept fixed. We imposed the symmetry constraint on the fit: The H atoms of the water moiety are symmetric with respect to the aromatic plane. Table V shows the results.

The O–O hydrogen bond length decreases by 5.0 pm upon electronic excitation, imaging the increased acidity of *p*-cresol upon electronic excitation, while the OOC angle and the HOOC dihedral, describing the orientation of the water

TABLE V. Structural r_0 parameters of *p*-cresol water. The atomic numbering refers to Fig. 1, the subscript *w* refers to atoms of the water moiety. The dihedral angle is defined between the H_1 atom of the water moiety, the O atom of water, the O_7 atom of cresol, and the C_1 atom of cresol. The second dihedral angle is determined by the symmetry constraint.

	$r(O_wO_7)$ (pm)	290.0(2)
	$a(O_wO_7C_1)$ (°)	114.4(12)
S_0	$a(H_{w1}O_wO_7C_1)$ (°)	120(47)
	$a(H_{w2}O_wO_7C_1)$ (°)	−120(47)
	$r(O_wO_7)$ (pm)	285.0(2)
	$a(O_wO_7C_1)$ (°)	113.9(20)
S_1	$a(H_{w1}O_wO_7C_1)$ (°)	116(16)
	$a(H_{w2}O_wO_7C_1)$ (°)	−116(16)
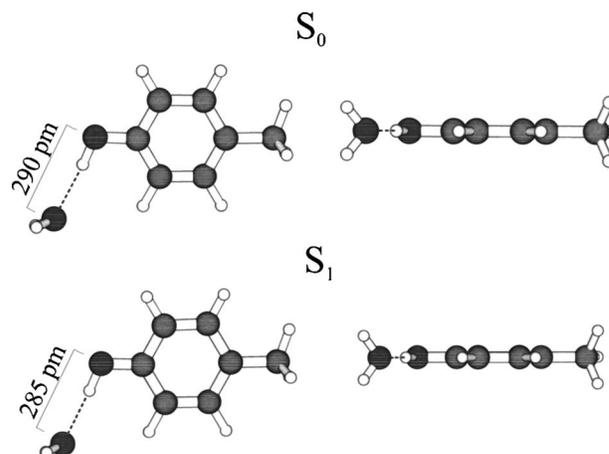
FIG. 5. Top and side views of the ground and excited state structures of *p*-cresol water. For all other geometry parameters see Table V.

moiety, nearly stay constant. Two different views of the ground and excited state structure are shown in Fig. 5.

VI. CONCLUSIONS

The value for the torsional barrier due to the internal rotation of the hydroxy group in *p*-cresol was found to be 1130 cm^{-1} in the ground state and 4395 cm^{-1} in the excited state. These values can be compared to the V_2 barriers of other *p*-disubstituted phenols and of phenol itself, given in Table VI.

Relative to phenol, *para* substitution with fluorine (+mesomeric effect) and methyl (+inductive effect) leads to a decrease of the torsional barrier in both electronic states, while the cyano group (−mesomeric effect) increases the barrier. Electron accepting groups (as cyano) stabilize a partial quinoidal structure of the *p*-substituted phenol with some double bond characters of the CO bond, while electron donating groups destabilize it. The lifetime of 4-methyl[7-*D*]phenol determined from the Lorentz contribution to the Voigt profile (9.7 ns) is substantially longer than the respective 4-methylphenol lifetime of 1.6 ns. A similar increase of the S_1-state lifetime was found for phenol and [7*D*]phenol and was explained by a smaller probability for tunneling of the OD species through the barrier which separates the $^1\pi\sigma^*$ from the $^1\pi\pi^*$ surface.[33]

The V_3 and V_6 barriers of the methyl-group torsion are low, as is typical for molecules with G_{12} symmetry. Barriers determined from 4-methylphenol and 4-methyl[7-*D*]phenol are equal within the uncertainty, showing that the two torsional motions are mainly decoupled.

TABLE VI. OH-torsional barriers of phenol, *p*-fluorophenol, *p*-cyanophenol, and *p*-methylphenol (*p*-cresol). All values are in cm^{-1}.

	V_2 barrier		
	S_0	S_1	References
p-fluorophenol	1006	1819	1
p-methylphenol	1130	4395	This work
phenol	1215	4710	17
p-cyanophenol	1420	>5000	2

From the rotational constants of both isotopomers, the structural change upon electronic excitation could be determined. As it is typical for *para*-disubstituted aromatics, the ring expands quinoidally upon excitation, while the two bonds in the *para* position decrease. The decrease of the CO bond length mirrors the shift of electron density from the oxygen atom to the aromatic ring, which takes place and is the reason for the increased acidity of phenols upon electronic excitation.

The rotationally resolved electronic spectrum of the origin of the water cluster is split into an $A^{(3)}E$ pair due to the methyl-group rotation and into an $A^{(2)}B$ pair due to the torsional motion of the water moiety. The S_1 lifetime of the *p*-cresol-water cluster determined from the Lorentz contribution to the Voigt profile is 42 ± 5 MHz, equivalent to a S_1-state lifetime of 3.8 ± 0.5 ns, which is much shorter than the lifetime of the similar phenol-water cluster (15 ns). The large increase of the lifetime by going from phenol to the phenol-water cluster was attributed by Sobolewski and Domcke to a removal of the conical intersection of the $^1\pi\sigma^*$ surface with the ground state. Furthermore, the $^1\pi\sigma^*$ surface shifts to higher energies, and develops a minimum at the hydrogen-transferred geometry of the cluster.[33] The longer lifetimes of deuterated phenol and the phenol-water cluster compared to phenol have therefore different explanations (smaller tunneling rate versus removal of a conical intersection). For the explanation of the lifetimes, it was also discussed that a rapid internal conversion takes place with the OH stretching vibration as an accepting mode.[34,35] Both deuteration and complexation with water lower the stretching frequency of the OH vibration, reducing its ability to act as an accepting mode. In this picture the lifetime of the *p*-cresol-water cluster should be equally increased as the one of deuterated *p*-cresol. However, we found a much shorter lifetime for the cresol-water cluster than for the deuterated cresol, strongly favoring the lifetime model of Sobolewski and Domcke.[33]

The structure of the *p*-cresol-water cluster could be determined to be *trans*-linearly hydrogen bound, with cresol as proton donor like in the similar phenol-water cluster. The OO hydrogen bond length could be determined to be 290 pm in the ground state and to 285 pm in the electronically excited state. This decrease in hydrogen bond length is a consequence of the increased acidity of *p*-cresol in the S_1 state, which leads to a stronger hydrogen bond. Again, the decrease of the hydrogen bond length of 5 pm is very similar to the corresponding value in phenol water (4 pm).

ACKNOWLEDGMENTS

[1] C. Ratzer, M. Nispel, and M. Schmitt, Phys. Chem. Chem. Phys. **5**, 812 (2002).

[2] J. Küpper, M. Schmitt, and K. Kleinermanns, Phys. Chem. Chem. Phys. **4**, 4634 (2002).

[3] M. Schmitt, C. Ratzer, C. Jacoby, and W. L. Meerts, J. Mol. Struct. **742**, 123 (2005).

[4] C. Ratzer, J. Küpper, D. Spangenberg, and M. Schmitt, Chem. Phys. **283**, 153 (2002).

[5] W. L. Meerts, M. Schmitt, and G. Groenenboom, Can. J. Chem. **82**, 804 (2004).

[6] Z. Arp, D. Autrey, J. Laane, S. A. Overman, and G. J. Thomas, Biochemistry **40**, 2522 (2001).

[7] M. Blomberg and P. Siegbahn, Mol. Phys. **101**, 323 (2001).

[8] G. Varsanyi, *Assignments for Vibrational Spectra of 700 Benzene Derivatives* (Wiley, New York, 1974).

[9] R. J. Jacobsen, Spectrochim. Acta **21**, 433 (1965).

[10] J. Laane, K. Haller, S. Sakurai, K. Morris, D. Autrey, Z. Arp, W. Chiang, and A. Combs, J. Mol. Struct. **650**, 57 (2003).

[11] T. Ebata and M. Ito, J. Phys. Chem. **96**, 3224 (1992).

[12] K. Song and J. M. Hayes, J. Mol. Spectrosc. **134**, 82 (1989).

[13] J. L. Lin, C. Li, and W. B. Tzeng, J. Chem. Phys. **120**, 10513 (2004).

[14] P. R. Richardson, M. A. Chapman, D. C. Wilson, S. P. Bates, and A. C. Jones, J. Chem. Phys. **4**, 4910 (2002).

[15] M. Pohl, M. Schmitt, K. Wolf, and K. Kleinermanns, J. Chem. Phys. **94**, 1717 (1991).

[16] M. Pohl, M. Schmitt, and K. Kleinermanns, Chem. Phys. Lett. **177**, 252 (1991).

[17] G. Berden, W. L. Meerts, M. Schmitt, and K. Kleinermanns, J. Chem. Phys. **104**, 972 (1996).

[18] M. Schmitt, J. Küpper, D. Spangenberg, and A. Westphal, Chem. Phys. **254**, 349 (2000).

[19] J. Küpper, Ph.D. thesis, Heinrich-Heine-Universität, Düsseldorf, 2000.

[20] W. Gordy and R. L. Cook, *Microwave Molecular Spectra*, 3rd ed. (Wiley, New York, 1984).

[21] C. C. Lin and J. D. Swalen, Rev. Mod. Phys. **31**, 841 (1959).

[22] D. R. Herschbach, J. Chem. Phys. **31**, 91 (1959).

[23] J. A. Hageman, R. Wehrens, R. de Gelder, W. L. Meerts, and L. M. C. Buydens, J. Chem. Phys. **113**, 7955 (2000).

[24] D. Levine, PGAPACK V1.0, PGAPACK can be obtained via anonymous ftp from ftp.mcs.anl.gov/pub/pgapack/ pgapack.tar.z., 1996.

[25] J. H. Holland, *Adaption in Natural and Artificial Systems* (University of Michigan Press, Ann-Arbor, MI, 1975).

[26] D. E. Goldberg, *Genetic Algorithms in Search, Optimisation and Machine Learning* (Addison-Wesley, Reading, Massachusetts, 1989).

[27] I. Rechenberg, *Evolutionsstrategie—Optimierung Technischer Systeme Nach Prinzipien der Biologischen Evolution* (Frommann-Holzboog, Stuttgart, 1973).

[28] C. Jacoby and M. Schmitt, ChemPhysChem **5**, 1686 (2004).

[29] M. Schmitt, Ph.D. thesis, Ruprecht-Karl-Universität, Heidelberg, 1992.

[30] A. Hellweg, in *Mikrowellenspektroskopische Untersuchungen zur intramolekularen Dynamik von p-Toluidin, p-Kresol und p-Thiokresol*, edited by Günter Mainz (Verlag Gýnter Mainz, Aachen, 2003).

[31] R. M. Helm, H. P. Vogel, and H. J. Neusser, J. Chem. Phys. **108**, 4496 (1998).

[32] K. Remmers, W. L. Meerts, and I. Ozier, J. Chem. Phys. **112**, 10890 (2000).

[33] A. L. Sobolewski and W. Domcke, J. Phys. Chem. A **105**, 9275 (2001).

[34] A. Sur and P. M. Johnson, J. Chem. Phys. **84**, 1206 (1986).

[35] R. J. Lipert and S. D. Colson, J. Phys. Chem. **93**, 135 (1989).